

# Remote Sensing for Maritime Monitoring and Vessel Characterization

Marco Reggiannini

*Institute of Information Science and Technologies*

*National Research Council of Italy*

Pisa, Italy

marco.reggiannini@isti.cnr.it

**Abstract**—The main objective of the work described here concerns the development of automatic ICT procedures in charge of processing imagery data captured by satellite-borne sensors to assess the status of a given maritime area. The mentioned assessment may refer to the detection and identification of peculiar objects, such as oil leaks or, in case of maritime traffic control, the recognition of navigating vessels. This paper specifically focuses on the development of methods for estimating the kinematics of a navigating vessel through the detection and analysis, in the 2D satellite imagery, of the corresponding wake pattern. The proposed method differentiates from those retrieved in previous literature for the introduction of a novel preprocessing stage, which allows for an enhancement in the overall performance of the wake detector. The resulting procedure represents a key functionality to be included in platforms dedicated to sea surveillance.

**Index Terms**—Maritime surveillance, SAR, Wake detector

## I. INTRODUCTION

Marine surface monitoring represents a task of paramount relevance to ensure marine traffic safety, malicious activity counteraction and timely intervention in case of emergency circumstances. Indeed it provides crucial information to be exploited for decision making purposes and to deal with a wide range of critical issues such as vessel traffic supervision or illegal fishery and pollution monitoring. To this purposes several joint research actions have been previously undertaken in order to develop solutions to issues related to maritime monitoring (see for instance [1]–[6]). Within this framework, the present paper reports about the development of automatic procedures for processing imagery captured by remote sensing devices.

In particular the discussed set of procedures constitutes a specific stage of the maritime monitoring software platform developed in the OSIRIS<sup>1</sup> project. The OSIRIS platform (see section V for details) can be operated as the cascade sequence of task-oriented stages, each involving the execution of specialized computer vision modules. The input data correspond to Synthetic Aperture Radar (SAR) and Optical maps captured by satellite-borne sensors (Sentinel-1A/B, Cosmo-Sky Med, EROS-B). These data feed a pipeline of processing steps devoted to i) the detection of targets (e.g. vessels) in the input map, ii) the extraction of the most descriptive features of candidate targets and finally iii) the estimation of peculiar

properties of candidate targets, properties that may represent crucial information to concerned operators (e.g. estimation of the dimensions of a vessel, of its route and velocity). The software steps that are preliminary applied concern the enhancement of the captured data in terms of signal-to-noise ratio. Indeed, the first goal when surveying maritime areas through remote sensing platforms, is to reduce the noise contaminations that typically affect the signal, such as speckle noise in case of SAR imaging systems. Once the visual enhancement has been carried out (see [7] for details), the signal is processed to perform the recognition in the maps of potential targets of interest and the analysis of their shape properties. This stage of the pipeline is dedicated to the extraction of visual attributes associated to the detected targets, aiming at providing a set of quantitative descriptors to be employed for classification purposes. In relation to this, the author has been concerned in detail with the implementation of an algorithm devoted to the estimation of the kinematics of detected targets. Concerning the vessel traffic monitoring system, this has been obtained through the automated analysis of the wake patterns observed in the image areas surrounding the target. In particular, the algorithm aims at i) detecting wake patterns generated by the ship's motion, ii) identify the wake components and estimate the route and, finally, iii) estimate the vessel's velocity based on the exploitation of imaging features related to the wake pattern components. The rest of the paper will focus on the specification of a method for the estimation of the vessel's speed obtained through the analysis of quasi-raw data, such as single-look-complex SAR maps. The paper is arranged as follows: section II concerns a brief State of the Art concerning previous literature approaches for ship kinematics estimation purposes, section III describes the author's approach to this topic, in section IV some results are discussed and section V is dedicated to the conclusions and potential future prospects.

## II. STATE OF ART

Several methods have been proposed to deal with the issue of estimating the kinematics of ship motion captured through SAR imaging systems. As previously mentioned the approach adopted in this work is based on the recognition and the analysis of the wake pattern generated by a vessel moving on the water surface (see Figure 1). A rigorous description

<sup>1</sup><http://wiki.services.eoportal.org/tiki-index.php?page=OSIRIS>

of the physics underlying the wake generation problem has been provided by previous eminent research [8]–[10]. For our purposes it is relevant to remark that the imaging attributes of such pattern are essentially related to the velocity of the vessel over the sea surface, and that these are mapped in SAR images by features related, in turn, to the velocity vectors (over ground) of the vessel and the satellite platform. Accordingly, popular approaches to kinematics estimation from SAR exploit the detection followed by the analysis of the wake.

Since wakes appear mainly as V-shaped forms, many have proposed detectors based on the preliminary recognition of linear segments. Zilman et al. [11] proposed a method based on the fast discrete Radon transform to detect the linear segments that start from the wake tip and develop along the wake shape. A similar approach has been adopted by Eldhuset [12], who introduced an approximation stage of the Radon transform based on the exploitation of the Chebyshev polynomials. This allows the author to enhance the detector performance in terms of reliability and robustness against false alarms.

The detected linear components of the wake are later analysed to estimate the ship's heading and the ship's velocity. According to [13]–[15], this can be obtained by performing proper analysis of the signal variations within the detected linear regions.

### III. PROPOSED METHOD

The proposed method is based on a few hypothesis which are here briefly discussed. First of all it is assumed that each moving vessel has a velocity vector that coincides with the principal axis of the hull, identified by the stern-bow oriented segment. Another basic assumption concerns the angular aperture between the wake most external arms, a morphological parameter which is expected to have a constant value for every observation. This hypothesis is effective for a certain range of velocities (from a few up to tens of km/h; see for example [16]), and for a variety of vessels' typologies with different hull dimensions. That said, the most relevant discriminating factors between wakes generated by different vessels are to be sought in the spatial frequency spectrum of the wake oscillations.

Generally speaking, a wake pattern in a SAR map is usually observed as the composition of three macro-structures that develop along linear directions: (i) a central turbulent strip, usually appearing as two collinear lines, a bright one next to a dark one, behind the vessel, with the same orientation of the vessel's heading and (ii) two linear bright stripes, located approximately at the wake boundaries, about  $\theta_{\pm} = \pm 19.47^\circ$  with respect to the central turbulent wake, in the so-called cusp wave regions of the wake. The angular aperture of the resulting V-shaped pattern features a constant value approximating  $39^\circ$ .

The key element of the proposed method is represented by the detection of the wake linear components, but it differs from similar classical approaches due to the integration in the pipeline of a novel process for Signal-to-Noise Ratio (SNR) enhancement (see section III-D). Once the wake pattern has been recognized, its internal components are analyzed to

extract features that enable to estimate the kinematics of the ship. To this purpose relevant features related to the motion of the ship are (i) the displacement between the vessel target and the wake tip, called Azimuth shift (only observed in SAR), and (ii) the spatial wavelength of the plane wave oscillation located at the edge sector of the wake envelope (*Kelvin wake*).

The processing steps that the algorithm goes through (pictorially illustrated in Figure 2) are discussed in the following sections.

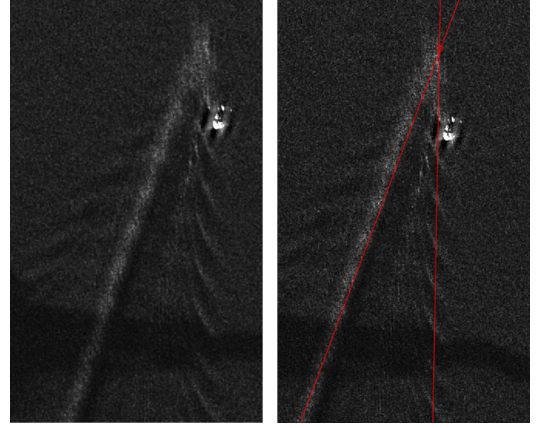


Fig. 1. Wake pattern detection. (COSMO-SkyMed Product—© ASI 2016 processed under license from ASI—Agenzia Spaziale Italiana, all rights reserved, distributed by e-GEOS (City, US State abbrev. if applicable, Country).

#### A. Ship Masking and Data Preprocessing

Due to very low SNR values ship wakes are usually not visible or too faint to be detected in SAR imagery. To the purpose of limiting false positive detections, the captured data must be preliminary processed to filter out noise or to

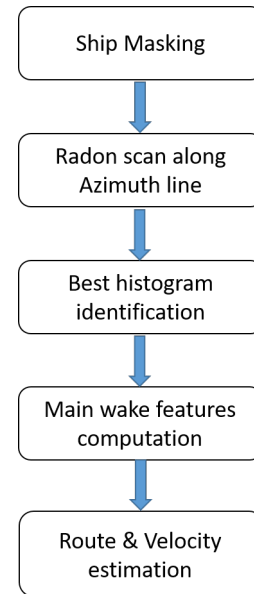


Fig. 2. Conceptual diagram of the vessel kinematics estimation.

neglect known spurious signals. For example pixels associated to the main vessel's body are excluded from the subsequent stages of the processing pipeline by exploiting the processing methods described in [17]. In a nutshell the ship's footprint is first estimated through a dedicated segmentation stage. Then pixels belonging to the ship's footprint (usually featuring large backscattering signals) are substituted by properly chosen intensity values (e.g. mean image intensity), so as to avoid those pixels to generate biased output from the subsequent linear detection stage.

### B. Azimuth Line Scan

As previously mentioned, in case of SAR remote sensing the tip of the wake generated by a moving object is represented in the map as displaced with respect to the object centroid by an amount of pixels, along the Azimuth direction and proportional to the object's velocity. This information is exploited to limit the domain for the wake tip search to the Azimuth line only (Figure 3).

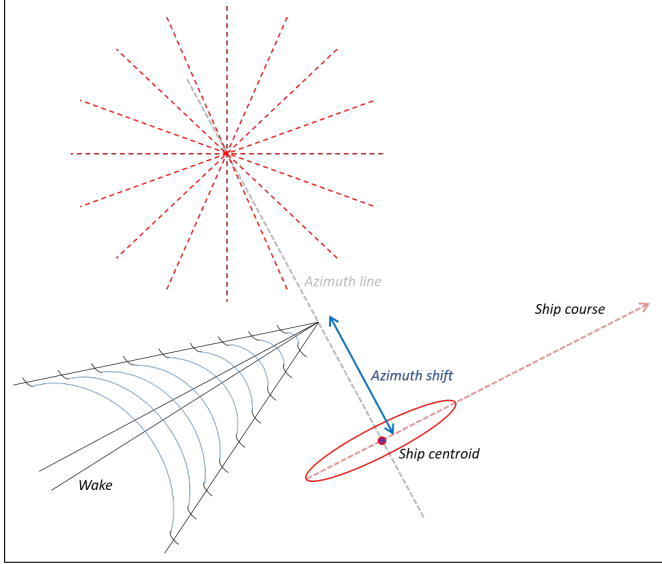


Fig. 3. Wake Pattern formation and representation in SAR remote sensing and punctual radon transform.

For each point  $p_j$  in image  $I$  such that it lies on the Azimuth line ( $j = 1, \dots, n_p$ , with  $n_p$  being the total number of points on the Azimuth line), consider the family of straight lines having  $p_j$  as the origin. Each line is univocally defined by an orientation angle  $\phi_i$  and has  $n_i$  pixels. Then the average image intensity along each line is computed. In case a  $1^\circ$  angular pace is set, we will have 360 lines starting from each  $p_j$ , and accordingly  $n_p$  angular histograms  $h_{p_j}(\phi_i)$  defined in  $1^\circ \leq \phi_i \leq 360^\circ$ :

$$h_{p_j}(\phi_i) = \frac{1}{n_i} \sum_{k=1}^{n_i} I(p_k)$$

$$p_k \in I : \arctan \left[ \frac{(p_k - p_j)_y}{(p_k - p_j)_x} \right] = \phi_i \quad (1)$$

If a linear segment has its origin located in one of the  $n_p$  points, the sum procedure generates a peak in the corresponding  $h_p$  function, for the particular orientation  $\phi_i$  related to that segment. The same is expected to be observed in case a point  $p_j$  coincides with the tip  $p_t$  of a wake. In the latter case  $h_{p_j}(\phi_i)$  will exhibit a number of peaks as large as the number of observed wake arms. Hence, a criterion to select the most probable wake tip candidate, consists of selecting the point  $p_j$  on the Azimuth line (Figure 3) such that the corresponding angular histogram  $h_{p_j}(\phi_i)$  features the largest peak intensity value:

$$p_t : \max_j h_{p_j}(\phi_i). \quad (2)$$

Performing this operation on the data represented in Figure 1, left side, returns the histogram function in Figure 4.

### C. Wake Detection

In order to decide whether an angular histogram is related to a meaningful portion of a wake pattern arm or it is due to noise/spurious signals, the histogram  $h_{p_t}(\phi_i)$ , selected through equation (2), undergoes a dedicated refinement stage, following the ideas described in [12].

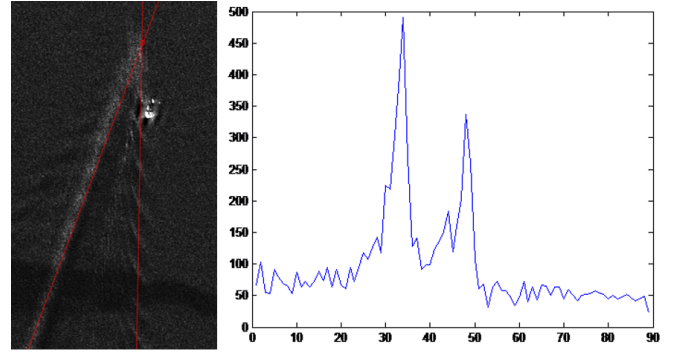


Fig. 4. Example of wake linear components detection resulting from the identification of the histogram with larger peak response. (COSMO-SkyMed Product—© ASI 2016 processed under license from ASI—Agenzia Spaziale Italiana, all rights reserved, distributed by e-GEOS.).

More in detail, the function  $h_{p_t}(\phi_i)$  is approximated, according to [18], by a linear combination  $g(\phi_i)$  of  $n$  Chebyshev polynomials, where  $n$  is the fit order and  $\phi_i \in [1^\circ, 360^\circ]$ . If  $n$  is chosen sufficiently small with respect to the number of histogram bins, e.g. selecting only the first few terms in the  $g$  series, the resulting fit will be a continuous curve that smoothly follows the input signal (see the example in Figure 5, where the approximated function, corresponding to the  $h_{p_t}$  function for this candidate, is identified by the red dotted curve).

Each point in the fit curve has an associated uncertainty which depends on the statistical hypothesis adopted to model the signal. According to the related literature (see for example [19]), SAR imagery capture is modeled as a speckle process and the corresponding pixel values are samples drawn from a Gamma distribution. Every point in the fit curve has a statistical deviation from the mean value,  $\sigma_i$ , that depends on

the number of samples  $n_i$  used to compute  $h_{p_i}(\phi_i)$  (see section III-B). Eventually, a candidate histogram  $h_{p_i}(\phi_i)$  is labeled as a wake positive detection in case one, or more, of its points, meaningfully overshoots a tolerance range defined by

$$h_{p_i}(\phi_i) \pm m\sigma_i \quad (3)$$

where  $m$  is an integer whose value is set according to the desired significance level of the detection. Since the tolerance range depends on  $\sigma_i$ , which varies from point to point, also the tolerance range has a varying width. To obtain the purple and yellow curves in Figure 5,  $m$  has been set to 3.5.

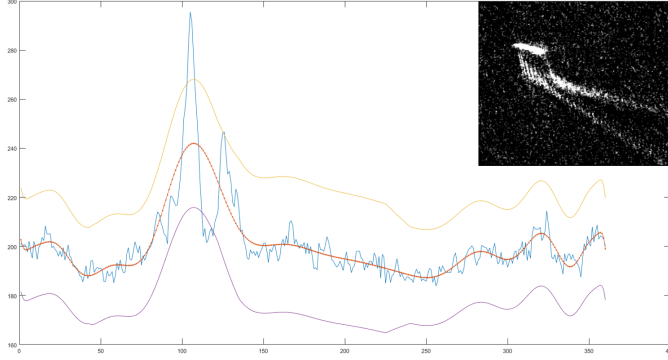


Fig. 5. Results of the Chebyshev polynomial fitting applied to the histogram obtained by processing the wake candidate in the top right corner. The fit order  $n$  has been set empirically to 30.

#### D. Gradient Based Wake Detection

This section concerns the description of a procedure for the image derivative estimation. This procedure is integrated in the wake detector processing pipeline aiming at the improvement of the detection robustness. The presented method for signal gradient computation turns out to be particularly suitable for speckle-affected signals.

Focusing on the wake central turbulent band, it is expected that the local gradient exhibits relevant variations moving along the direction orthogonal to the wake center axis (Figure 6). However, it is a proven fact (see [20]) that estimating the gradient through differences of standard masks (e.g.,  $[-1, 0, 1]$  or  $[-1, 0, 1]^T$ ) results in low performances on speckle-affected data.

In order to robustly estimate the signal gradient, the author adopted the approach described in [21], i.e. the signal derivative at a given point  $(x, y)$  has been computed through the ratio of average (*roa*) estimator (see Figure 7), which is defined, for the vertical and horizontal cases, as

$$roa_v(x, y) = \frac{\langle I_U \rangle}{\langle I_D \rangle}, \quad roa_h(x, y) = \frac{\langle I_L \rangle}{\langle I_R \rangle} \quad (4)$$

with  $\langle \dots \rangle$  representing the average operator. The vertical and horizontal *roa* correspond to the vertical and horizontal gradient components, obtained as:

$$\begin{aligned} G_V(x, y) &= \log(roa_v(x, y)), \\ G_H(x, y) &= \log(roa_h(x, y)) \end{aligned} \quad (5)$$

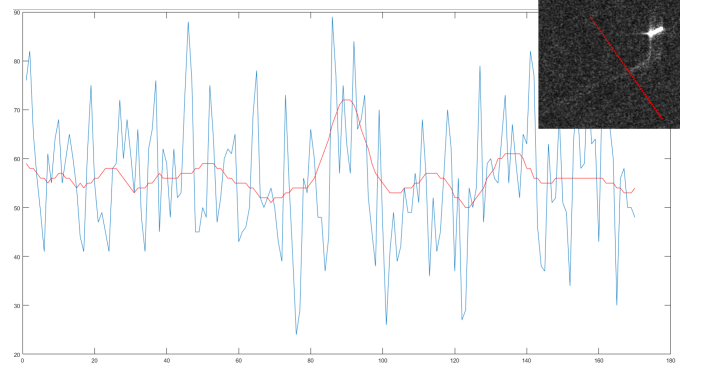


Fig. 6. SAR signal sampled along a direction orthogonal to the turbulent component of the wake, faintly visible in the small crop. The original signal is represented in blue color (sampled along the dotted line in the upper right patch) while the red curve represents the result of a Gaussian lowpass filtering, applied to reduce speckle noise. The turbulent wake corresponds to the bell-shaped signal in the range  $[80 \div 100]$ .

and the related magnitude and phase values

$$\begin{aligned} M_G(x, y) &= \sqrt{G_V(x, y)^2 + G_H(x, y)^2}, \\ \theta_G(x, y) &= \arctan\{G_V(x, y)/G_H(x, y)\} \end{aligned} \quad (6)$$

Hence, gradient phase and amplitude are estimated, for every pixel in the image, by means of Equations (5). Eventually, in order to capture and isolate the maximum variation of the signal in the wake neighborhood, the estimated gradient is projected onto the direction orthogonal to the previously estimated main axis of the ship. The robustly estimated gradient is later processed by the wake detection procedures discussed in sections III-B and III-C.

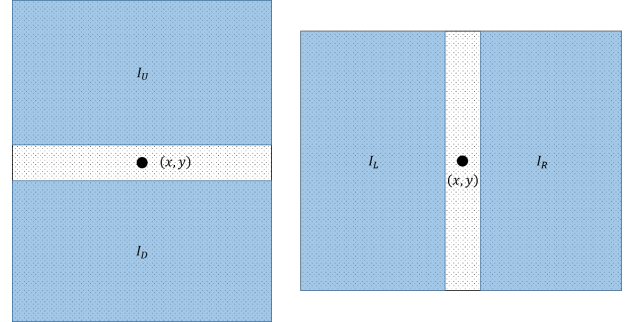


Fig. 7. Ratio of average computation along the vertical and horizontal directions.

#### E. Wake Analysis

In case a crop candidate passes the detection stage, it is further processed to extract the information that is considered of interest for the kinematics estimation. First of all, the peaks that overshoot the  $m\sigma_i$  threshold are identified as related to wake components. As already stated in [22], in the most favourable case, the observable wake components are the central turbulent band, coinciding with the vessel route, and two external envelopes placed symmetrically at  $\pm 19.47^\circ$  w.r.t. the wake center axis.



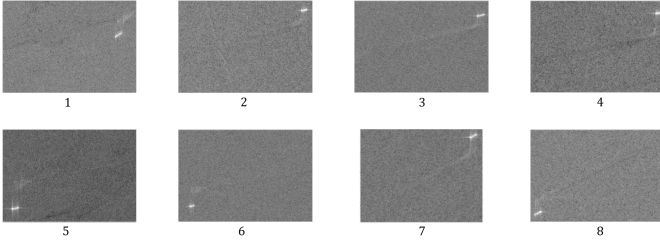


Fig. 8. Dataset employed to test the turbulent wake detector (contains modified Copernicus Sentinel data [2018]).

Since the vessel route coincides with the center band of the wake pattern, recognizing the turbulent component represents a crucial goal for the wake analysis task. In case the number of observed components is at a maximum, the route is defined as the bisector between the most external components, while, in case a single line is detected, this will be automatically identified as the turbulent component. In the most ambiguous circumstance, i.e., when the algorithm detects two different lines, the adopted approach consists of labeling the component that exhibits the largest mean value as the turbulent band. The choice for this criterion stems from the observation that the central turbulent band of a wake usually features the largest backscattering signal, hence the largest peak in the angular histogram can be linked to the wake central orientation.

After the vessel route estimation, the wake pattern is considered for estimating the ship's speed. The velocity estimation stage is carried out following approaches that have been already presented in previous literature and that make use of the ship motion's related features introduced in section III-A. For further details the reader is invited to refer to [7].

#### IV. RESULTS

The proposed turbulent wake detector has been applied to the dataset in Figure 8.

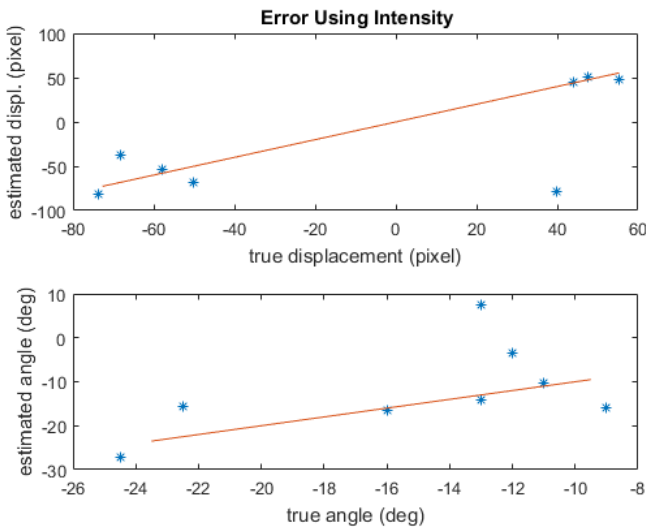


Fig. 9. Standard method error diagram.

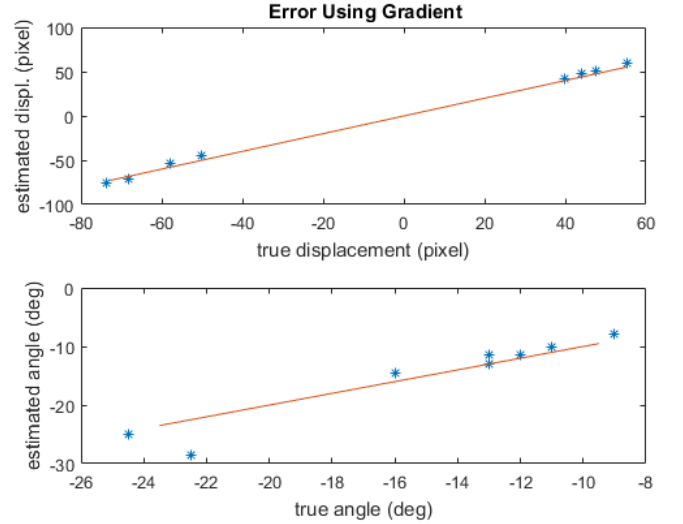


Fig. 10. Proposed method error diagram.

The corresponding error plots are represented in Figures 9 and 10, where the estimated Azimuth displacement and turbulent wake orientation have been plotted versus the corresponding true values. In particular, the first set of diagrams represents the comparison between true and estimated data, where the latter have been obtained by applying the proposed pipeline directly on the intensity maps (standard approach following [12], Figure 9), while the second set (Figure 10) accounts for the results obtained by preprocessing the intensity map by the method described in section III-D. It is relevant to consider the data dispersion around the red line (the  $y = x$  line) in Figure 10, and observe the higher performance of the proposed method w.r.t. the standard method (Figure 9).

Concerning the estimation of the target velocity the analysis of the wake pattern has been performed on the ship target represented in Figure 11. In this case, it has been possible to get reliable ground truth data from a commercial Automatic Identification System (AIS, [23]) provider. Velocity estimates are provided according to the methods described in [7], i.e., the method exploiting the Azimuth shift and the one exploiting the Fourier analysis performed on the external Kelvin wake. Concerning the latter method, the Fourier analysis has been performed on the main wake components, i.e. three lines starting from the wake tip (see Figure 12). The performed analysis provided the results in Table I where **AIS R** and **Est. R** stand for AIS Route and Estimated Route respectively, while **AIS V** stands for AIS Velocity. The presented velocity estimates correspond to the Azimuth Shift (**ASV**) method and to the Fourier Analysis method (**FAV**).

TABLE I  
KINEMATICS ESTIMATION OUTPUT

<b>AIS R</b>	<b>Est. R</b>	<b>AIS V</b>	<b>ASV</b>	<b>FAV</b>
290°	285°	6 m/s	5.89 m/s	6.22 m/s

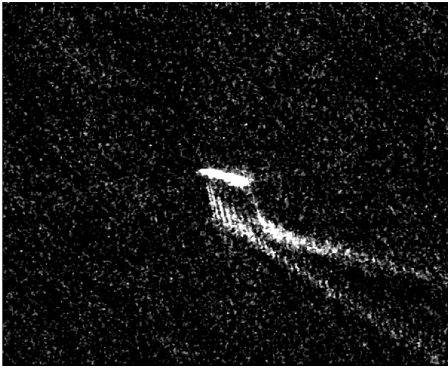


Fig. 11. Sample crop exploited for the kinematics estimation test reported in table I

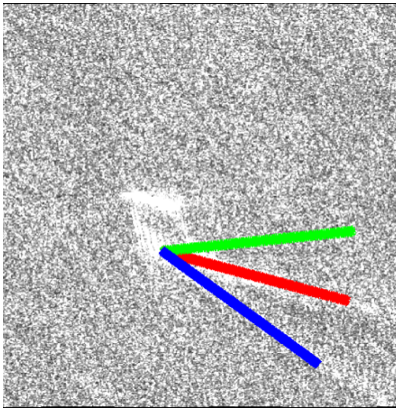


Fig. 12. Linear sampling on the wake signal presented in Figure 11. (COSMO-SkyMed Product—© ASI 2016 processed under license from ASI—Agenzia Spaziale Italiana, all rights reserved, distributed by e-GEOS.)

## V. CONCLUSIONS

This document presents the implementation and the results related to an image processing pipeline dedicated to the ship kinematics estimation task. This procedure takes as input remote sensing imagery and returns the estimated values of the vessel route and the vessel speed. This is primarily conceived to process radar imagery but can also be applied to optical data, provided some proper preliminary processing stages are introduced in order to enhance the wake pattern traces.

A novel method for the detection of the wake has been introduced. Promising results obtained by processing the dataset in Figure 8 suggest that employing the proposed gradient-based approach may enhance the accuracy concerning the estimation of the ship motion's related features (see charts in Figures 9 and 10).

Concerning future prospects, the author envisages developing novel procedures for wake detection, taking inspiration from cutting edge literature of machine learning. To this purpose particular interest will be devoted to the usage of deep convolutional networks, employed as a powerful tool for the extraction of discriminating features from large amounts of open access data (e.g., the ESA Copernicus Open Access Hub). Wake patterns are hardly detectable in SAR maps, hence

future developments will also be devoted to the refinement of the wake recognition process, based on the exploitation of additional information, such as the fine estimate of the vessel position as well as the constraints of this peculiar hydrodynamics problem, e.g. the theoretically expected wake angular aperture. For what concerns the estimation of the vessel's speed, novel methods are currently being investigated to evaluate their potential in terms of kinematics information extraction. In particular, along-track-interferometry techniques represent interesting tools for the purpose of estimating the line-of-sight velocity value through the analysis of single-look-complex SAR data. Moreover, the Doppler centroid of the SAR signal varies according to the kinematics of the backscatterer. Estimating the variation between the Doppler centroid of a moving object w.r.t. a stationary one provides an additional velocity estimation method, which sounds worthy of being further studied.

The presented platform has been tested within the framework of OSIRIS (Optical/SAR data and system Integration for Rush Identification of Ship models), a European Space Agency project with the main goal of developing a platform dedicated to sea surveillance, capable of detecting and identifying illegal maritime traffic. The main goal of this platform is to detect and identify target vessels within a given sea surface area, which is remotely supervised by orbiting satellites such as Sentinel 1/2, Cosmo-Sky Med and EROS missions. The most relevant goals that are addressed by this platform concern (i) the estimation of the ship positioning within the inspected area, (ii) the estimation of the main ship geometrical attributes (length overall, beam overall and heading) and (iii) the ship kinematics status represented by its velocity vector. OSIRIS will represent a new tool to counteract unauthorized fishing and tackle irregular migration and the related smuggling activities.

## REFERENCES

- [1] DOLPHIN Project <http://www.gmes-dolphin.eu> (accessed on 9 May 2019).
- [2] NEREIDS Project <https://cordis.europa.eu/project/rcn/99070/factsheet/en> (accessed on 9 May 2019).
- [3] SIMTISYS Project <https://cordis.europa.eu/project/rcn/99196/factsheet/en> (accessed on 9 May 2019).
- [4] PERSEUS Project <http://www.perseus-net.eu/site/content.php> (accessed on 9 May 2019).
- [5] AMASS Project <https://cordis.europa.eu/project/rcn/86259/factsheet/en> (accessed on 9 May 2019).
- [6] Santamaria, C., Stasolla, M., Fernandez Arguedas, V., Argentieri, P., Alvarez, M., Greidanus, H.: Sentinel-1 Maritime Surveillance: Testing and Experiences with Long-term Monitoring, <https://doi.org/10.2788/090400>, 2015.
- [7] Reggiannini, M.; Bedini, L.: Multi-Sensor Satellite Data Processing for Marine Traffic Understanding. *Electronics* **2019**, 8(2), 152.
- [8] Thomson, W. On the Waves Produced by a Single Impulse in Water of Any Depth, or in a Dispersive Medium. *Proc. R. Soc. Lond.* **1887**, 42, 80–83.
- [9] Tuck, E.O.; Collins, S.I.; Wells, W.H. On Ship Wave Patterns and Their Spectra. *J. Ship Res.* **1991**, 15, 11–21.
- [10] Crawford, F.S. Elementary Derivation of the Wake Pattern of a Boat. *Am. J. Phys.* **1984**, 51, 782–785.
- [11] Zilman, G.; Zapolski, A.; Marom, M. The speed and beam of a ship from its wakes SAR images. *IEEE Trans. Geosci. Remote Sens.* **2004**, 42, 2335–2343.

- [12] Eldhuset, K. An automatic ship and ship wake detection system for spaceborne SAR images in coastal regions. *IEEE Trans. Geosc. Remote Sens.* **1996**, *34*, 1010–1019.
- [13] Tunaley, J.K.E. The Estimation of Ship Velocity from SAR Imagery. In Proceedings of the 2003 IEEE International Geoscience and Remote Sensing Symposium, Toulouse, France, 21–25 July **2003**; Volume 1, pp. 191–193.
- [14] Scherbakov, A.; Hanssen, R.; Vosselman, G.; Feron, R. Ship wake detection using Radon transforms of filtered SAR imagery. *Proc. SPIE* **1996**, 2958, 96–106.
- [15] Graziano, M.D.; D’Errico, M.; Rufino, G. Ship Heading and Velocity Analysis by Wake Detection in SAR Images. *Acta Astronaut.* **2016**, *128*, 72–82.
- [16] Rabaud, M.; Moisy, F. Ship wakes: Kelvin or Mach angle? *Phys. Rev. Lett.* **2013**, *110*, 214503, doi:10.1103/PhysRevLett.110.214503.
- [17] Bedini, L.; Righi, M.; Salerno, E. Size and Heading of SAR-Detected Ships through the Inertia Tensor. *Proceedings* **2018**, *2*, 97.
- [18] Cheney, W.; Kincaid, D. *Numerical Mathematics and Computing*; Brooks/Cole: Monterey, CA, USA, **1980**.
- [19] Papoulis, A.; Pillai, S.U. : Probability, Random Variables, and Stochastic Processes. *McGraw Hill, 4th Edition*, **2002**.
- [20] Dellinger, F.; Delon, J.; Gousseau, Y.; Michel, J.; Tupin, F. SAR-SIFT: A SIFT-like Algorithm for SAR Images. *IEEE Trans. Geosci. Remote Sens.* **2015**, *1*, 453–466.
- [21] Song, S.; Xu, B.; Yang, J. SAR Target Recognition via Supervised Discriminative Dictionary Learning and Sparse Representation of the SAR-HOG Feature. *Remote Sens.* **2016**, *8*, 683, doi:10.3390/rs8080683.
- [22] Reggiannini, M.; Bedini, L. Synthetic Aperture Radar Processing for Vessel Kinematics Estimation. In Proceedings of the International Workshop on Computational Intelligence for Multimedia Understanding, IWCIM 2017, Kos, Greece, 2 September **2017**. Available online: <https://tinyurl.com/y79l38o7> (accessed on 28 January **2019**).
- [23] Automatic Identification System: <http://www.imo.org/en/OurWork/Safety/Navigation/Pages/AIS.aspx> (accessed on 28 January **2019**).